# Photon subtraction and addition by a three-level atom in an optical cavity

Julio Gea-Banacloche and William Wilson
*Department of Physics, University of Arkansas, Fayetteville, Arkansas 72701, USA*
(Received 3 May 2013; published 19 September 2013)

Rosenblum *et al*. showed recently that a three-level atom in a cavity can function as a perfect "photon turnstile." Here we explore how this device reshapes the incident pulses, generalize it to the case of an input coherent state, and consider its use in reverse as a "photon adder." We find that for initially unentangled pulses, adding one photon to an $|n\rangle$ number state is possible with a success probability equal to $1/(n+1)$.

DOI: 10.1103/PhysRevA.88.033832 PACS number(s): 42.50.Ct, 42.50.Pq, 42.50.Ex, 42.50.Dv

## I. INTRODUCTION

In a recent paper, Rosenblum *et al*. [1] have shown that a three-level atom inside a one-sided optical cavity, in the configuration sometimes called a "one-dimensional atom" [2], can function as a perfect "photon turnstile" (see [3–5] for various demonstrations of the photon turnstile concept). One may also think of it as a perfect "photon subtractor," which would turn an incident number state $|n\rangle$ of $n$ photons with a certain polarization, into the state $|n-1\rangle$, plus a single photon state with the orthogonal polarization.

The analysis in [1] was based on a concatenated cavity approach [6], so it was limited in its treatment of the incident pulse shapes. Here we use the general space-time treatment for quantized fields interacting with cavities, developed in [7] (see also [8,9] for equivalent approaches), to obtain closed-form analytical expressions for the output pulses valid for arbitrarily shaped input pulses, in the adiabatic limit. We also present numerical results for Gaussian pulses (for the $n=2$ case) showing the effect of working away from adiabaticity, and extend the treatment to input coherent states. The latter results are particularly interesting, since they show that this system, with a "classical" field input, can become a near-deterministic source of single photons on demand; the fact that the classical field in this scheme is fed through the cavity mirror, rather than through the sides, may make it easier to implement experimentally than, e.g., the system demonstrated in [10].

Finally, we consider the possible use of the one-dimensional atom in reverse, as a photon adder. We find that, for initially unentangled pulses, the photon addition only works probabilistically, but one can in principle get an $n+1$ photon pulse with the same profile as the input pulses (containing $n$ and 1 photons in orthogonal polarization states, respectively) with probability $1/(n+1)$. Hence this system may also be a useful source of small-number Fock states, a problem that has also been the subject of much interest lately [11–13].

## II. THE PHOTON SUBTRACTION SCHEME

### A. Basic equations

The system we will consider is illustrated in Fig. 1. There is a single, three-level atom (in the $\Lambda$ configuration) inside a one-sided optical microcavity. The two atomic transitions (assumed degenerate; see below) couple to two orthogonal polarizations of light, which here we take to be horizontal and vertical for definiteness, although they could also be right and left circular. We assume the coupling to the cavity is strong enough for spontaneous emission out the sides of the cavity to be negligible. A polarizing beam splitter may be used to combine or separate few-photon pulses with orthogonal polarizations.

We use the space-time description presented in [7]. The general Hamiltonian has the form

$$H = -i\hbar g \int \frac{\sqrt{\kappa/\pi}}{\kappa - i\omega}(|e\rangle\langle g_h|a_\omega + |e\rangle\langle g_v|b_\omega)e^{-i(\omega+\delta)t}\,d\omega + \text{H.c.} \tag{1}$$

Here the operators $a_\omega$ and $b_\omega$ annihilate horizontally and vertically polarized photons, respectively, and obey continuum commutation relations: $[a_\omega, a^\dagger_{\omega'}] = \delta(\omega-\omega')$. The frequencies $\omega$ are measured from the cavity frequency $\Omega_c$ (that is, if $\Omega$ is the actual field frequency, $\omega = \Omega - \Omega_c$), and $\delta = \Omega_c - \omega_a$ is the detuning of the cavity from the atom. As is customary in cavity quantum electrodynamics, the parameter $g$ (equal to one-half of the "vacuum" or "one-photon" [14] Rabi frequency) denotes the strength of the coupling between the atomic transition and the cavity mode, which we take to be the same for both transitions. The parameter $\kappa$ is the cavity amplitude decay rate for the field, here assumed to be entirely due to transmission through the input mirror (see Sect. IV for further comments on these and other assumptions).

We write the overall state at any time as

$$|\Psi(t)\rangle = |\psi_h(t)\rangle|g_h\rangle + |\psi_v(t)\rangle|g_v\rangle + |\psi_e\rangle|e\rangle, \tag{2}$$

where the field states $|\psi_h(t)\rangle, \ldots$ are defined as $\langle g_h|\Psi(t)\rangle, \ldots$. They satisfy the coupled equations

$$\frac{d}{dt}|\psi_e\rangle = -g\sqrt{\frac{\kappa}{\pi}}\int \frac{1}{\kappa - i\omega}(a_\omega|\psi_h\rangle + b_\omega|\psi_v\rangle)e^{-i(\omega+\delta)t}\,d\omega, \tag{3a}$$

$$\frac{d}{dt}|\psi_h\rangle = g\sqrt{\frac{\kappa}{\pi}}\int \frac{1}{\kappa + i\omega}a^\dagger_\omega|\psi_e\rangle e^{i(\omega+\delta)t}\,d\omega, \tag{3b}$$

$$\frac{d}{dt}|\psi_v\rangle = g\sqrt{\frac{\kappa}{\pi}}\int \frac{1}{\kappa + i\omega}b^\dagger_\omega|\psi_e\rangle e^{i(\omega+\delta)t}\,d\omega. \tag{3c}$$

We will assume that the atom-cavity detuning is zero, and that the pulse is also resonant with the cavity, so the frequencies $\omega$ appearing in Eqs. (3) are centered around zero. Then, if the pulse duration $T$ is very long, so that $\kappa T \gg 1$ and adiabatic following takes place, we can assume that the frequencies which contribute significantly to the integrals in (3) are always very small compared to $\kappa$. All our calculations below will be based on this adiabatic approximation [note that this, by itself,

 

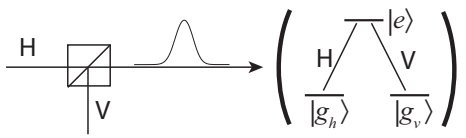


FIG. 1. The "one-dimensional three-level atom" considered in this paper (see text for details).

does not require either the "bad" ($\kappa > 2g$) or "good" ($\kappa < 2g$) cavity limit to apply].

Neglecting $\omega$ versus $\kappa$ in all the denominators in Eqs. (3), we formally integrate Eqs. (3b) and (3c) and substitute in (3a):

$$\frac{d}{dt}|\psi_e\rangle = -\frac{g^2}{\kappa\pi}\int_0^t dt' \int d\omega \int d\omega' [a_\omega a^\dagger_{\omega'}|\psi_e(t')\rangle + b_\omega b^\dagger_{\omega'}|\psi_e(t')\rangle] e^{-i(\omega t-\omega' t')} - \frac{g}{\sqrt{\kappa\pi}}\int [a_\omega|\psi_h(0)\rangle + b_\omega|\psi_v(0)\rangle] e^{-i\omega t}\, d\omega. \quad (4)$$

For the photon subtraction scenario we will assume that initially we have only $N$ horizontally polarized photons, and zero vertically polarized ones. Then the last term in (4) is zero, and also, there are no vertically polarized photons in the state $|\psi_e(t)\rangle$. Then, if we use Eq. (2) to put (4) in normal order, we get

$$\frac{d}{dt}|\psi_e\rangle = -\Gamma|\psi_e\rangle - \Gamma\int_0^t dt'\, A^\dagger(t')A(t)|\psi_e(t')\rangle - \sqrt{\Gamma}A(t)|\psi_h(0)\rangle, \quad (5)$$

where the "bad cavity" characteristic decay rate $\Gamma = 2g^2/\kappa$ has been introduced, and the operator $A(t)$ is defined as

$$A(t) = \frac{1}{\sqrt{2\pi}}\int a_\omega e^{-i\omega t}\, d\omega \quad (6)$$

satisfying

$$[A(t), A^\dagger(t')] = \delta(t-t'). \quad (7)$$

As shown by Rosenblum *et al.* [1], the perfect photon turnstile is obtained in the adiabatic limit, when the pulse is very long compared to $1/\Gamma$. We thus require $2g^2T/\kappa \gg 1$ in addition to the previous condition $\kappa T \gg 1$. In this limit, Eq. (5) can be simplified to

$$|\psi_e\rangle \simeq -\int_0^t dt'\, A^\dagger(t')A(t)|\psi_e(t')\rangle - \frac{1}{\sqrt{\Gamma}}A(t)|\psi_h(0)\rangle, \quad (8)$$

an implicit equation for $|\psi_e\rangle$ that can be solved by iteration. Substituting the right-hand side of (8) back in itself, we obtain

$$|\psi_e\rangle = -\frac{1}{\sqrt{\Gamma}}A(t)|\psi_h(0)\rangle + \frac{1}{\sqrt{\Gamma}}\int_0^t dt'\, A^\dagger(t')A(t)A(t')|\psi_h(0)\rangle + \int_0^t dt' \int_0^{t'} dt''\, A^\dagger(t')A(t)A^\dagger(t'')A(t')|\psi_e(t'')\rangle. \quad (9)$$

If we use the commutator (7) to put the last term of (9) in normal order, we find that the integral over $t''$ of the term proportional to $\delta(t-t'')$ vanishes for all $t'$ except when $t' = t$, where it has a finite value. The integral (over $t'$) of a finite function that is zero almost everywhere is zero, so this term does not contribute and we can simply rewrite (9) as

$$|\psi_e\rangle = -\frac{1}{\sqrt{\Gamma}}A(t)|\psi_h(0)\rangle + \frac{1}{\sqrt{\Gamma}}\int_0^t dt'\, A^\dagger(t')A(t)A(t')|\psi_h(0)\rangle + \int_0^t dt' \int_0^{t'} dt''\, A^\dagger(t')A^\dagger(t'')A(t)A(t')|\psi_e(t'')\rangle. \quad (10)$$

Now we can continue the iteration by substituting (8) into (10), and again rewriting the result in normal order introduces no extra terms. We clearly end up with the series

$$|\psi_e\rangle = -\frac{1}{\sqrt{\Gamma}}\Big[A(t)|\psi_h(0)\rangle - \int_0^t dt'\, A^\dagger(t')A(t)A(t')|\psi_h(0)\rangle + \int_0^t dt' \int_0^{t'} dt''\, A^\dagger(t')A^\dagger(t'')A(t)A(t')A(t'')|\psi_h(0)\rangle + \cdots\Big], \quad (11)$$

which terminates after $N$ terms for an initial $N$-photon state. This can be used back in (3b) and (3c) to determine the final state.

### B. $N$-photon initial wave packet

An $N$-photon initial wave packet can be described by

$$|\psi_h(0)\rangle = |N\rangle \equiv \frac{1}{\sqrt{N!}}\left(\int \tilde{f}(\omega)a^\dagger_\omega\, d\omega\right)^N |0\rangle, \quad (12)$$

where, by normalization, the function $\tilde{f}(\omega)$ must satisfy $\int |\tilde{f}(\omega)|^2\, d\omega = 1$. It is straightforward to see that

$$A(t)|N\rangle = \sqrt{N}\,\frac{1}{\sqrt{2\pi}}\int \tilde{f}(\omega)e^{-i\omega t}\, d\omega\, |N-1\rangle = \sqrt{N}\, f(t)|N-1\rangle, \quad (13)$$

where the function $f(t)$, defined by the above equation and also normalized to unity, gives the pulse profile. We assume throughout that at the initial time $t = 0$, one has $f(t) \simeq 0$; that is, the initial time $t = 0$ is chosen to be long before the pulse reaches the cavity. With this assumption, the result (12) and repeated integration by parts can be used to reduce the series Eq. (11) to the closed form

$$|\psi_e\rangle = \frac{1}{\sqrt{\Gamma}}\, f(t)\sum_{n=1}^{N}(-1)^n\sqrt{\frac{N!}{(N-n)!}} \times \frac{1}{(n-1)!}\left(\int_0^t f(t')A^\dagger(t')dt'\right)^{n-1}|N-n\rangle. \quad (14)$$

If the function $f(t)$ is negligible for $t < 0$, the lower limit of integration can be formally taken to be $-\infty$ in Eq. (14). It can then be simplified further by noting that

$$|N-n\rangle = \frac{1}{\sqrt{(N-n)!}}\left(\int_{-\infty}^{\infty} f(t')A^\dagger(t')\, dt'\right)^{N-n}|0\rangle \quad (15)$$

since the time integral in this expression simply produces the frequency components $\tilde{f}(\omega)$ appearing in Eq. (12). Substituting (15) in (14) and using the binomial theorem then yields

$$|\psi_e\rangle = -\frac{\sqrt{N}}{\sqrt{(N-1)!}}\frac{f(t)}{\sqrt{\Gamma}}\left(\int_t^\infty f(t')A^\dagger(t')dt'\right)^{N-1}|0\rangle. \tag{16}$$

This can now be used in Eq. (3b) to calculate the part of the final state associated with finding the atom in the $|g_h\rangle$ ground state. In the adiabatic limit, and with $\delta = 0$, Eq. (3b) can be written as

$$\frac{d}{dt}|\psi_h\rangle = \sqrt{\Gamma}A^\dagger(t)|\psi_e(t)\rangle. \tag{17}$$

Clearly, by inspection, this equation is satisfied by

$$|\psi_h(t)\rangle = \frac{1}{\sqrt{N!}}\left(\int_t^\infty f(t')A^\dagger(t')dt'\right)^N|0\rangle \tag{18}$$

since its derivative equals the right-hand side of (17), and its value at $t = 0$ [same as $t = -\infty$ if $f(t)$ is negligible for $t < 0$] is the correct $N$-photon state $|N\rangle$ [according to Eq. (15), with $n = 0$].

It follows immediately from Eq. (18) that $|\psi_h(\infty)\rangle = 0$. Hence, in this (adiabatic) limit the atom makes the transition to the other ground state with unit probability, and a single vertically polarized photon is certain to be produced. The field state is then given by $|\psi_v(\infty)\rangle$, which is obtained by integrating the equation (3c):

$$\frac{d}{dt}|\psi_v\rangle = \sqrt{\Gamma}B^\dagger(t)|\psi_e(t)\rangle. \tag{19}$$

Here the operator

$$B(t) = \frac{1}{\sqrt{2\pi}}\int b_\omega e^{-i\omega t}\,d\omega \tag{20}$$

has been defined for the vertically polarized modes, by analogy to $A(t)$. Substituting Eq. (16) in (19), the result for the final field state is then

$$|\psi_v(\infty)\rangle = -\frac{\sqrt{N}}{\sqrt{(N-1)!}}\int_{-\infty}^\infty dt'\, f(t')B^\dagger(t') \times\left(\int_{t'}^\infty f(t'')A^\dagger(t'')dt''\right)^{N-1}|0\rangle. \tag{21}$$

Note that, in general, the vertically polarized ($v$ for short) photon is quite entangled with the horizontally polarized ($h$) photons.

The joint probability to detect a $v$ photon at the space-time point $\tau_1$ and an $h$ photon at $\tau_2$ (where $\tau$ can be, for instance, $t - z/c$, for a pulse traveling to the right) is proportional to the expectation value of the operator $B^\dagger(\tau_1)B(\tau_1)A^\dagger(\tau_2)A(\tau_2)$ in the state (21). This can be calculated by using the commutation relations to move all the annihilation operators to act on the vacuum state. The result is

$$I_{vh}(\tau_1,\tau_2) \propto N(N-1)|f(\tau_1)|^2|f(\tau_2)|^2\theta(\tau_2-\tau_1) \times\left(\int_{\tau_1}^\infty |f(t')|^2dt'\right)^{N-2}, \tag{22}$$

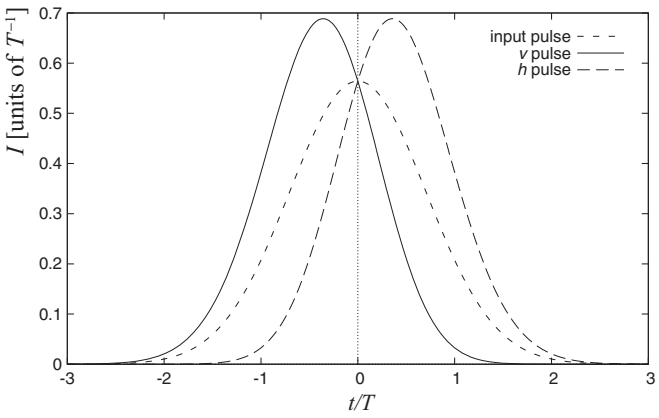


FIG. 2. The incoming pulse with $N = 2$ horizontally polarized photons (short-dashed line), and the outgoing single-photon $v$ pulse (solid line) and $N - 1$ photon $h$ pulse (long-dashed line). Time is in units of $T$; if $|f|^2$, $I_h$, and $I_v$ are interpreted as probability distribution functions, the vertical axis is in units of $1/T$.

where $\theta$ is the Heaviside theta function. This shows that it is impossible to detect an $h$ photon before a $v$ photon, a very strong correlation already pointed out by Rosenblum *et al.* This is a feature of the adiabatic approximation and does not generally hold in other regimes, as seen in Fig. 8 below. Formally it is due to the fact that in (21) the creation operators for the $h$ photons only act after the $v$ photon is created; this, in turn, follows directly from the form (16) of $|\psi_e(t)\rangle$, which ultimately must result from the interference between all the absorption and reemission processes indicated in expression (11).

Integrating (22) over $\tau_2$ gives the unconditioned distribution for the $v$ photon:

$$I_v(\tau_1) = N|f(\tau_1)|^2\left(\int_{\tau_1}^\infty |f(t')|^2dt'\right)^{N-1} \tag{23}$$

[here normalized to unity by dividing out the factor $N - 1$ which appears on the right-hand side of Eq. (22)], whereas integrating over $\tau_1$ gives the distribution for $h$ photons:

$$I_h(\tau_2) = N\,|f(\tau_2)|^2\left[1-\left(\int_{\tau_2}^\infty |f(t')|^2dt'\right)^{N-1}\right], \tag{24}$$

which in this form is normalized to $N - 1$. Note $I_h(\tau_2) = N|f(\tau_2)|^2 - I_v(\tau_2)$, so in some sense the wave packet for the $N - 1$ $h$ photons is obtained by subtracting from the incoming wave packet (with an appropriate weight factor) the wave packet for the single $v$ photon. Alternatively, we can say that the sum of the two unconditioned distributions equals the original one, normalized to the original number of photons $N$.

These results are illustrated in Figs. 2–5 for an initial Gaussian pulse with a profile given by

$$|f(t)|^2 = \frac{1}{T\sqrt{\pi}}e^{-t^2/T^2} \tag{25}$$

[note that the quantity $T$ used here to characterize the duration of a Gaussian pulse is different from the $T$ used in previous papers such as [7]; one has $T$ (this paper) $= T_{\rm prev}/\sqrt{2}$].

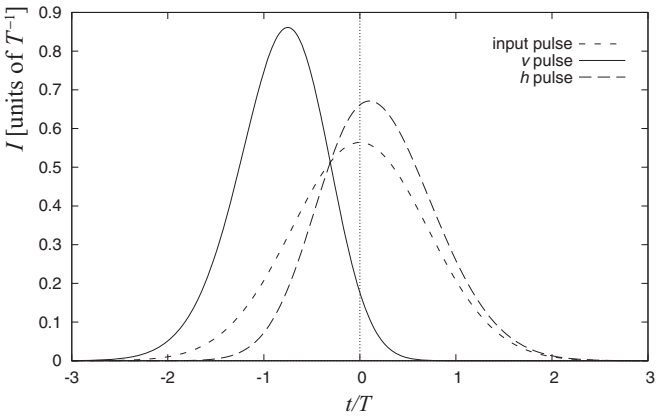


FIG. 3. Same as in Fig. 2, for $N = 5$.

Equations (23) and (24) become

$$I_v(t) = \frac{N}{2^{N-1}T\sqrt{\pi}}\, e^{-t^2/T^2}\left[1 - \mathrm{erf}\left(\frac{t}{T}\right)\right]^{N-1},$$
$$I_h(t) = \frac{N}{T\sqrt{\pi}}\, e^{-t^2/T^2}\left\{1 - \frac{1}{2^{N-1}}\left[1 - \mathrm{erf}\left(\frac{t}{T}\right)\right]^{N-1}\right\}. \quad (26)$$

Note that this has a very symmetric form for $N = 2$, as shown in Fig. 2.

For larger $N$, in Figs. 3 and 4 we have plotted $I_h/(N-1)$, since this is normalized to unit area. Clearly as the number of photons in the original pulse increases, the removal of one photon has less and less of an effect, and asymptotically, for large $N$, $I_h$ just approaches $|f(t)|^2$. The single-photon $v$ pulse, on the other hand, starts appearing earlier and earlier, and it also becomes narrower.

This behavior of the $v$-photon pulse with increasing $N$ can be qualitatively understood as follows. First, note that in this adiabatic (or very-fast-cavity) limit, the photon absorption and emission processes are essentially instantaneous. This can be seen by taking $N = 1$ in Eq. (23): The probability to get a $v$ photon is in that case at every moment directly proportional to the probability (given by $|f(t)|^2$) for the $h$ photon to just be there. Similarly, in the $N > 1$ case, all it takes to generate the $v$ photon is for one of the $N$ $h$ photons to be present in the cavity. As $N$ increases, this becomes more and more likely for earlier times. This explains the shifting of the pulse towards

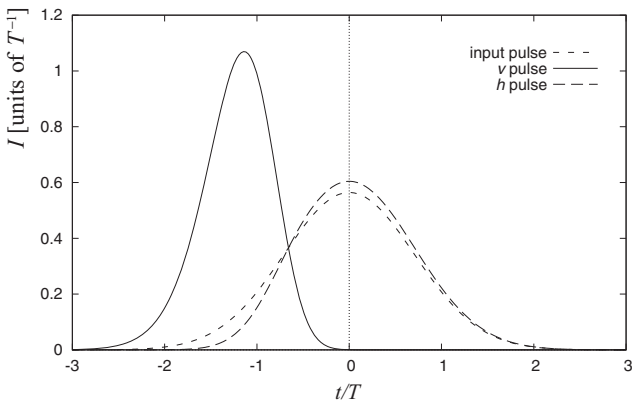


FIG. 4. Same as in Fig. 2, for $N = 15$.

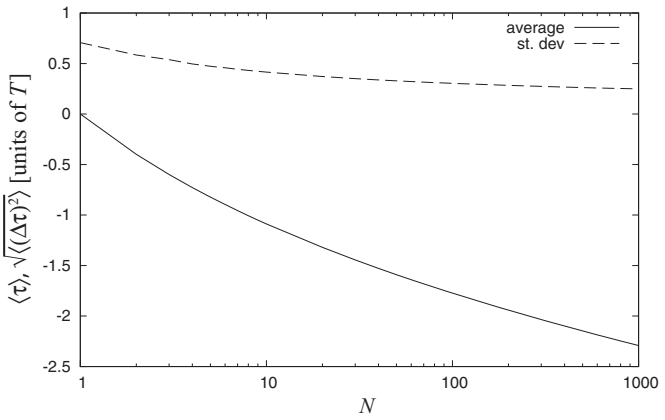


FIG. 5. Average (solid line) and standard deviation (dashed line) of the distribution $I_v(t)$ as a function of $N$ (in units of $T$).

earlier times. Also, note that the $v$ pulse should go to zero once it becomes all but certain that a $v$ photon has been emitted, which is to say as soon as it is all but certain that at least one $h$ photon has arrived at the atom. The more photons one has, the earlier this happens also, and hence the earlier the $v$ pulse goes to zero. Finally, the narrowing happens because with more photons available it takes comparatively less time to reach that certainty.

The narrowing of the $v$ pulse may cause some concern that the adiabatic approximation may become invalid for large $N$, but fortunately the effect is a very slow function of $N$. Figure 5 shows the numerically calculated average and standard deviation of the function $I_v$, in units of $T$, as a function of $N$. Note that even for $N = 1000$, the standard deviation is still $\sim 0.25T$, or about $0.25\sqrt{2} = 0.35$ times what it was for the incoming pulse. As Fig. 5 shows, the shift of the pulse towards earlier times is a more substantial effect.

### C. Numerical results for $N = 2$

The results in the previous section are expected to be valid in the doubly adiabatic limit $\kappa T \gg 1$, $\Gamma T \gg 1$. It is possible to check this numerically in the simplest case of a two-photon $h$ pulse ($N = 2$). We have used a discrete-mode approximation to the Hamiltonian (1) (see [7] for details).

Figure 6 shows contour lines for the error probability $1 - P_v$, defined as the probability that the atom may *not* end up in the $|g_v\rangle$ state. The lines have been drawn at logarithmic intervals, so error probability decreases by a factor of 2 from one line to the next. As expected, it is not enough to just make one of $\kappa T$ and $\Gamma T$ large, but moderate values of both actually suffice to make $1 - P_v$ relatively small. For instance, $\kappa T = 4$, $gT = 4$ is enough to get $\Gamma T = 8$ and a failure probability of 0.0118 [15].

Figure 7, calculated for these values of $\kappa T$ and $\Gamma T$, shows that even for these very low failure probabilities there is still some visible disagreement between the numerically calculated pulses and the theoretical results derived in the previous section, although, as expected, we find that the agreement improves as $\kappa T$ and $\Gamma T$ increase. For smaller values of these parameters, we may find much more dramatic disagreement. For instance, for $\kappa T = 4$ but $gT = 1$ (which means $\Gamma T = 0.5$) one obtains the result in Fig. 8, which shows the vertical pulse

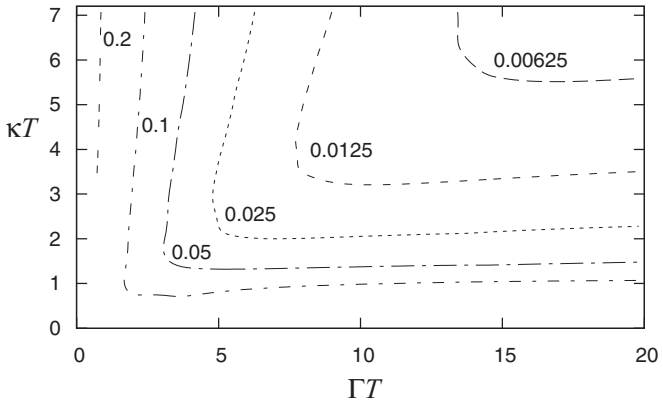


FIG. 6. Contour lines for the error probability $1 - P_v$, calculated numerically for $N = 2$.

coming out *after* the horizontal one (the failure probability, that is, the probability that there may, in fact, be no vertical pulse, is about 0.26, or 1/4, in this case).

### D. Initial coherent state pulse

A multimode coherent state is typically written as

$$|\alpha\rangle = \prod_k |\alpha_k\rangle, \tag{27}$$

where the index $k$ runs over a (discrete, for convenience) set of modes. The total average number of photons is

$$\bar{n} = \langle\alpha| \left( \sum_k a_k^\dagger a_k \right) |\alpha\rangle = \sum_k |\alpha_k|^2 \tag{28}$$

and the pulse shape is given by the probability to detect a photon at the space-time point $\tau$, which, as usual, goes as

$$\begin{aligned} I(t) \;&\propto \frac{c}{L} \langle\alpha| \left( \sum_k a_k^\dagger e^{i\omega_k \tau} \right) \left( \sum_{k'} a_{k'} e^{-i\omega_{k'}\tau} \right) |\alpha\rangle \\ &= \frac{c}{L} \left| \sum_k \alpha_k e^{-i\omega_k \tau} \right|^2 \equiv \bar{n} |f(\tau)|^2, \end{aligned} \tag{29}$$

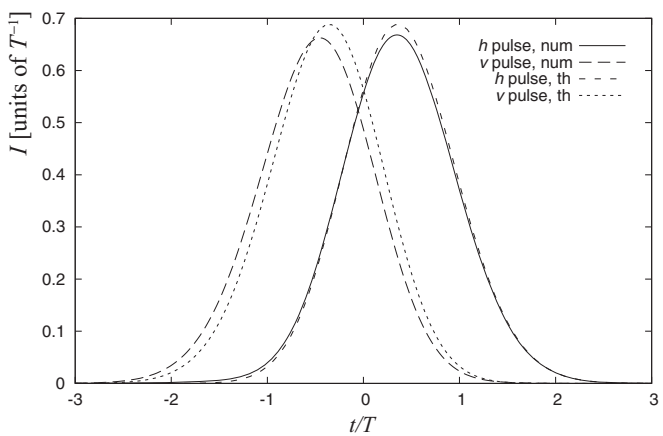


FIG. 7. Numerically calculated results for $I_h$ and $I_v$, compared to the asymptotic predictions Eq. (27), for $\kappa T = gT = 4$.

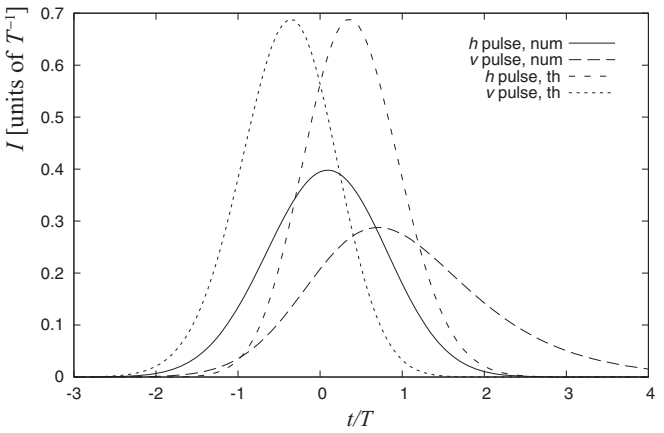


FIG. 8. Numerically calculated results for $I_h$ and $I_v$, compared to the asymptotic predictions Eq. (27), for $\kappa T = 4, gT = 1$ ($\Gamma T = 0.5$).

where $L$ is the quantization length and the function $f(\tau) = \sqrt{c/L} \sum_k \alpha_k e^{-i\omega_k \tau}/\sqrt{\bar{n}}$ has unit norm over the interval $L/c$, according to (28). Clearly, the state (27) can alternatively be written as

$$\begin{aligned} |\alpha\rangle &= e^{-\sum_k |\alpha_k|^2/2} e^{\sum_k \alpha_k a_k^\dagger} |0\rangle \\ &= e^{-\bar{n}/2} \sum_{n=0}^{\infty} \frac{\bar{n}^{n/2}}{n!} \left( \sum_k \frac{\alpha_k}{\sqrt{\bar{n}}} a_k^\dagger \right)^n |0\rangle \\ &= e^{-\bar{n}/2} \sum_{N=0}^{\infty} \frac{\bar{n}^{N/2}}{\sqrt{N!}} |N\rangle. \end{aligned} \tag{30}$$

This is just a superposition of multimode number states of the same form as the ones appearing in Eq. (12), only for a discrete set of modes; however, the continuum limit in Eq. (30) poses no problems. The essential point is that for all the $|N\rangle$ states, the pulse profile is given by the same function $f(\tau)$, proportional to the Fourier transform (discrete or continuous) of the amplitudes $\alpha_k$, and normalized to unity over an interval that may be extended to $(-\infty, \infty)$.

All the states in the sum (30) with $N \geqslant 1$ will be transformed according to Eq. (21), so the final state of the field associated with the $|g_v\rangle$ state of the atom will be

$$\begin{aligned} |\psi_v(\infty)\rangle = -e^{-\bar{n}/2} \sqrt{\bar{n}} \int_{-\infty}^{\infty} dt' \, f(t') B^\dagger(t') \\ \times \exp\left( \sqrt{\bar{n}} \int_{t'}^{\infty} f(t'') A^\dagger(t'') \, dt'' \right) |0\rangle. \end{aligned} \tag{31}$$

Once again, this is a highly entangled state. For each value of $t'$, the state of the $h$ field is a coherent state with a different (complex) amplitude, whereas the corresponding state of the $v$ field is a one-photon state. The norm of (31) is not, in general, equal to 1, since there is a probability equal to $e^{-\bar{n}}$ that the initial state of the field may have been the vacuum, in which case the atom will not transition to the state $|g_v\rangle$. The failure probability of the photon subtraction scheme with a coherent state input is therefore equal to $e^{-\bar{n}}$.

The $v$ pulse shape can be obtained most simply by adding the probabilities (23) with the appropriate weights, given by (30). Once again, the sum can be carried out, with the

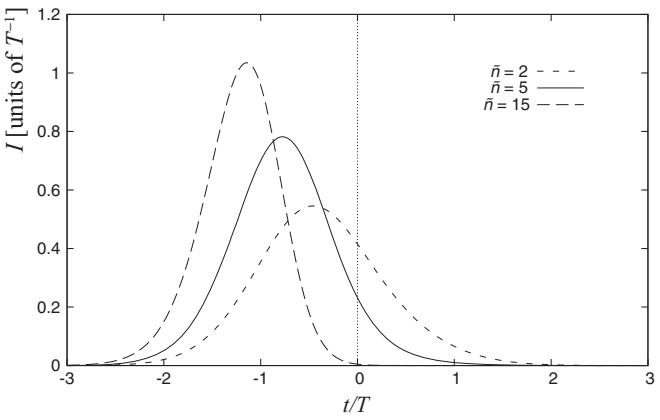


FIG. 9. Single-photon $v$-polarized pulses generated from $h$-polarized coherent states with $\bar{n} = 2$, 5, and 15, respectively.

result

$$I_v(\tau_1) = e^{-\bar{n}}\bar{n}|f(\tau_1)|^2 \exp\left(\bar{n}\int_{\tau_1}^{\infty}|f(t')|^2\,dt'\right) = \bar{n}|f(\tau_1)|^2 \exp\left(-\bar{n}\int_{-\infty}^{\tau_1}|f(t')|^2\,dt'\right). \quad (32)$$

It is easy to see by direct calculation that this indeed integrates to $1 - e^{-\bar{n}}$, confirming our expectations for the failure probability.

For the Gaussian pulses considered earlier [Eq. (25)], this becomes

$$I_v(t) = \frac{\bar{n}}{T\sqrt{\pi}}\exp\left\{-\frac{t^2}{T^2} - \frac{\bar{n}}{2}\left[1 + \mathrm{erf}\left(\frac{t}{T}\right)\right]\right\}. \quad (33)$$

The single-photon $v$ pulses corresponding to $\bar{n} = 2$, 5, and 15 are shown in Fig. 9. Note that they do not look significantly different from the ones generated from initial number states (Figs. 2–4). Their areas give their probabilities, and as indicated above, they are given by the general formula $1 - e^{-\bar{n}}$; they are 0.865, 0.993, and 1.0 (to six significant figures), respectively. Hence, coherent states (classical pulses) with as few as five photons on average could be used in this scheme as effective near-deterministic generators of single-photon pulses.

## III. PHOTON ADDITION

It is tempting to think that one could run the photon subtractor in reverse, so that an input of one $v$ photon and $N$ $h$ photons would be converted into a number state with $N + 1$ $h$ photons; one could then generate large number states in this way. Unfortunately, since the subtractor's output states (21) are highly entangled, the reverse operation will not work for initially unentangled pulses; or, rather, it will only work probabilistically.

The description of the "photon adder" starts with the same equations (3), but different initial conditions. Referring to Eq. (4), now we assume that $|\psi_h(0)\rangle$ is zero (the atom starts in the $|g_v\rangle$ ground state). As before, however, there are no $v$ photons in the state $|\psi_e(t)\rangle$, so after putting (4) in normal order we get

$$\frac{d}{dt}|\psi_e\rangle = -\Gamma|\psi_e\rangle - \Gamma\int_0^t dt'\,A^\dagger(t')A(t)|\psi_e(t')\rangle - \sqrt{\Gamma}B(t)|\psi_v(0)\rangle. \quad (34)$$

The same methods as in Sec. II A can be used to derive the equivalent of Eq. (11):

$$|\psi_e\rangle = -\frac{1}{\sqrt{\Gamma}}\Bigg[B(t)|\psi_h(0)\rangle - \int_0^t dt'\,A^\dagger(t')A(t)B(t')|\psi_h(0)\rangle + \int_0^t dt'\int_0^{t'} dt''\,A^\dagger(t')A^\dagger(t'')A(t)A(t')B(t'')|\psi_h(0)\rangle + \cdots\Bigg]. \quad (35)$$

Assuming that the initial state consists of a pair of number states, with (in general) different temporal profiles,

$$|\psi_h(0)\rangle = \frac{1}{\sqrt{N!}}\left(\int\tilde{h}(\omega)b_\omega^\dagger\,d\omega\right)\left(\int\tilde{f}(\omega)a_\omega^\dagger\,d\omega\right)^N|0\rangle, \quad (36)$$

one obtains

$$|\psi_e(t)\rangle = -\frac{1}{\sqrt{\Gamma}}\Bigg[h(t)|N\rangle_h - \sqrt{N}\,f(t)\int_0^t dt'\,A^\dagger(t')h(t')|N-1\rangle_h + \sqrt{N(N-1)}\,f(t)\int_0^t dt'\,A^\dagger(t')f(t') \times\int_0^{t'} dt''\,A^\dagger(t'')h(t'')|N-2\rangle_h + \cdots\Bigg]|0\rangle_v. \quad (37)$$

This can now be substituted in Eq. (3b), and integrated from 0 to $t$; the integration interval can be extended to $(-\infty,\infty)$ as before, to obtain the final state of the system, and then repeated integration by parts can be used to bring all the $h$'s to the front:

$$|\psi_h(\infty)\rangle = -\int_{-\infty}^{\infty}A^\dagger(t)h(t)dt\Bigg[|N\rangle_h - \sqrt{N}\int_t^{\infty}dt'\,A^\dagger(t')f(t')|N-1\rangle_h + \sqrt{N(N-1)}\int_t^{\infty}dt'\,A^\dagger(t')f(t') \times\int_{t'}^{\infty}dt''\,A^\dagger(t'')f(t'')|N-2\rangle_h + \cdots\Bigg]|0\rangle_v, \quad (38)$$

which can be put in the compact form

$$|\psi_h(\infty)\rangle = -\frac{1}{\sqrt{N!}}\int_{-\infty}^{\infty}h(t)A^\dagger(t)dt \times\left(\int_{-\infty}^{t}f(t')A^\dagger(t')\,dt'\right)^N|0\rangle. \quad (39)$$

It is now easy to see that, if $h = f$,

$$|\psi_h(\infty)\rangle = -\frac{1}{\sqrt{N+1}}\,|N+1\rangle_h|0\rangle_v \quad [h(t) = f(t)], \tag{40}$$

that is, the photon is removed from the $v$ mode and added to the $h$ mode, but only with a probability $1/(N+1)$. This is already as small as 0.5 for $N = 1$ (generation of a two-photon state), and only gets smaller as $N$ increases.

On the other hand, the advantage of the choice $h = f$ is that the resulting pulse has the same profile as the incoming ones. Also, in any case, the failure to produce the state (39) is heralded: One only needs to look for the original $v$ photon in the output state to know that the conversion did not take place. So we could produce two-photon states with probability $1/2$, and know when we have succeeded (of course, only if we have unit efficiency photon detectors); then, given a one-photon and a two-photon state, we could make a three-photon state with probability $1/3$, and so on. As long as one does not need a number state with a lot of photons, these odds are probably tolerable.

Alternatively, one could try to choose $f$ and $h$ so as to maximize the conversion probability, but this comes at the cost of having to deal with differently shaped pulses at every stage of the process.

## IV. FEASIBILITY

The main constraint that needs to be satisfied to implement this scheme is the doubly adiabatic condition $\kappa T, \Gamma T \gg 1$. In addition to this we have made a number of simplifying assumptions, some of which also amount to experimental requirements; these include neglecting spontaneous emission in out-of-cavity modes, degenerate atomic transitions, and equal couplings for both transitions. Also, cavity losses other than transmission through the input mirror have also been neglected.

Since the hope was expressed in the Introduction that the design presented here might simplify the implementation of some optical-cavity-based single-photon sources, such as Ref. [10], by eliminating the need to excite the atom with an external beam through the side of the cavity, we may take the cavity parameters of [10] as a starting point for a feasibility discussion. For this experiment, involving a cesium atom, McKeever *et al.* reported $g/2\pi = 16$ MHz, $\kappa/2\pi = 4.2$ MHz, $\gamma$ (spontaneous emission rate) $= 2.6$ MHz. From this we get $\Gamma = 2g^2/\kappa = 122/2\pi$ MHz. Under these conditions (compare Fig. 6), a $T$ of the order of $3 \times 10^{-7}$ s should suffice to ensure very high conversion efficiency. This can be done with the atom held in place in a trap, as in [10], or even with an atom freely falling through the cavity, as in the experiments reported in [16], where transit times of the order of 100 $\mu$s were reported.

As for the effect of spontaneous emission, if we assume the atom is only excited for a time of the order of $1/\Gamma$, the associated error probability would be of the order of

$$\frac{\gamma}{\Gamma} = \frac{\kappa\gamma}{2g^2}, \tag{41}$$

which is equal to 0.02 for the above parameters.

A more significant problem for high-finesse optical microcavities are absorption and scattering losses at the mirrors, which are typically not negligible compared to the transmission losses [17]. If we write the total decay rate of a photon in the cavity as $\kappa_{\text{trans}} + \kappa_{\text{abs}}$, then the photon lifetime in the cavity is of the order of $1/(\kappa_{\text{trans}} + \kappa_{\text{abs}})$, and the probability that it may be absorbed in this time is $\kappa_{\text{abs}}/(\kappa_{\text{trans}} + \kappa_{\text{abs}})$, which according to [17] may be as large as 0.4, or 40%. This is a potentially serious difficulty, since it essentially turns the photon generation into a random (as opposed to a near-deterministic) process, but clearly any scheme based on these types of high-finesse optical cavities would be afflicted by the same problem.

Alternatives to conventional Fabry-Perot microcavities certainly exist (see, for instance, the review [18]), and there are studies that indicate that, for instance, for dielectric microspheres below a certain size the losses are overwhelmingly dominated by radiative processes [19], so such systems (which still can reach very large quality factors) may be better suited for practical single-photon sources. For such systems, their ability to channel spontaneous emission into the cavity mode is often characterized by the so-called Purcell number $P$; for a Fabry-Perot cavity, $1/P$ is essentially the same as the quantity (41) above. For microposts and micropillars, Vahala [18] quotes Purcell factors in the 10–100 range.

For many of these solid-state systems, a better source of photons might be a quantum dot, instead of a three-level atom. Then our scheme requires a way to get a three-level, $\Lambda$ configuration in a quantum dot. This has been the subject of numerous studies, beginning with the work of Imamoğlu *et al.* [20]; as a relatively recent reference, we mention [21]. We are not really knowledgeable enough about these systems to venture a guess as to how easy or hard it may be to realize the present scheme in them.

Regarding some of our other assumptions, unequal couplings $g$ (or, more precisely, $\Gamma$) for the two atomic transitions do degrade the performance of our scheme, but not very dramatically. Interestingly, this is an error that *decreases* with increasing $N$. By redoing the calculations in Sec. II with different $\Gamma_h$ and $\Gamma_v$, one obtains an error probability [basically, the norm squared of $|\psi_h(\infty)\rangle$] given by

$$P_e = \left(\frac{\Gamma_h - \Gamma_v}{\Gamma_h + \Gamma_v}\right)^{2N}. \tag{42}$$

For example, if $\Gamma_h = 1.5\Gamma_v$, then $P_e = 0.04, 0.0016$, and $6.4 \times 10^{-5}$ for $N = 1$, 2, and 3, respectively. We believe this is because for classical fields the adiabatic following that takes the atom from one ground state to another is "exact" (for an infinitely slow pulse) regardless of the magnitude of the couplings.

For an atom in free space, if the ground states merely correspond to different values of the $z$ component of the total angular momentum, the transitions should be automatically degenerate, and the couplings to the orthogonal polarizations identical, by global rotational symmetry. However, in many cases, in practice, one may want to break the degeneracy (for instance, with an external magnetic field). Nondegenerate transitions and unequal couplings also arise naturally in quantum dot systems.

For quantum logical gates based on this system (originally proposed in [22]) the consequences of dealing with

nondegenerate atomic transitions have been explored quite thoroughly in [23]. For the simpler use suggested here, they do not, in fact, pose a problem; all that is required is to set the cavity frequency halfway between the two atomic transitions, so that the effective coupling to both modes, $g^2\kappa/(\kappa^2+\Delta^2)$, be the same (it might also be possible to use different values of $\Delta_h$ and $\Delta_v$ to compensate in part for different values of $g_h$ and $g_v$). The fields should still be resonant with the atomic transitions themselves, which means that the different polarizations would also have different frequencies in this case.

## V. CONCLUSIONS

The results presented here add to the already impressive list of useful properties of this "one-dimensional three-level atom" setup. It has the potential to serve for storing the state of a single photonic qubit [24], to mediate photon-photon gates that enable universal quantum computing [22], to function as an effectively deterministic source of single-photon pulses, with a "classical field" input, and to generate probabilistically, but in a heralded way, Fock states of relatively low numbers of photons. A photonic quantum computer could, in principle, be built entirely out of these basic modules, plus appropriate optical elements and photon routers.

## ACKNOWLEDGMENT

This research has been supported by the National Science Foundation.

[1] S. Rosenblum, S. Parkins, and B. Dayan, Phys. Rev. A **84**, 033854 (2011).
[2] Q. A. Turchette, R. J. Thompson, and H. J. Kimble, Appl. Phys. B **60**, S1 (1995).
[3] J. Kim, O. Benson, H. Kan, and Y. Yamamoto, Nature (London) **397**, 500 (1999).
[4] P. Michler, A. Kiraz, C. Becher, W. V. Schoenfeld, P. M. Petroff, L. Zhang, E. Hu, and A. Imamoğlu, Science **290**, 2282 (2000).
[5] B. Dayan, A. S. Parkins, T. Aoki, E. P. Ostby, K. J. Vahala, and H. J. Kimble, Science **319**, 1062 (2008).
[6] H. J. Carmichael, Phys. Rev. Lett. **70**, 2273 (1993).
[7] J. Gea-Banacloche, Phys. Rev. A **87**, 023832 (2013).
[8] K. Kojima, H. F. Hofmann, S. Takeuchi, and K. Sasaki, Phys. Rev. A **68**, 013803 (2003).
[9] K. Koshino and H. Ishihara, Phys. Rev. A **70**, 013806 (2004).
[10] J. McKeever, A. Boca, A. D. Boozer, R. Miller, J. R. Buck, A. Kuzmich, and H. J. Kimble, Science **303**, 1992 (2004).
[11] E. Waks, E. Dimanti, and Y. Yamamoto, New J. Phys. **8**, 4 (2006).
[12] M. Hofheinz *et al.*, Nature (London) **454**, 310 (2008); **459**, 546 (2009).
[13] K. Xia, G. K. Brennen, D. Ellinas, and J. Twamley, Opt. Express **20**, 27198 (2012).
[14] Both terms are used in the literature. For instance, [16] uses "single-photon Rabi frequency," whereas [18] uses "vacuum" Rabi frequency.
[15] Again, please note that in terms of the $T$ used in previous papers by J. G. B. and coauthors to characterize the pulse duration, this condition should be written as $\kappa T_{\rm prev} = gT_{\rm prev} = 4\sqrt{2}$.
[16] R. Miller, T. E. Northup, K. M. Birnbaum, A. Boca, A. D. Boozer, and H. J. Kimble, J. Phys. B **38**, S551 (2005).
[17] C. J. Hood, H. J. Kimble, and Jun Ye, Phys. Rev. A **64**, 033804 (2001).
[18] K. J. Vahala, Nature (London) **424**, 839 (2003).
[19] J. R. Buck and H. J. Kimble, Phys. Rev. A **67**, 033806 (2003).
[20] A. Imamoğlu, D. D. Awschalom, G. Burkard, D. P. DiVincenzo, D. Loss, M. Sherwin, and A. Small, Phys. Rev. Lett. **83**, 4204 (1999).
[21] A. Majumdar, Z. Lin, A. Faraon, and J. Vučković, Phys. Rev. A **82**, 022301 (2010).
[22] K. Koshino, S. Ishizaka, and Y. Nakamura, Phys. Rev. A **82**, 010301(R) (2010).
[23] J. Gea-Banacloche and L. M. Pedrotti, Phys. Rev. A **86**, 052311 (2012).
[24] G. W. Lin, X. B. Zou, X. M. Lin, and G. C. Guo, Europhys. Lett. **86**, 30006 (2009).